IMAGE QUALITY ASSESSMENT IN CMOS AND CR MEDICAL IMAGING SYSTEMS

Christoforos Ntales[1], Nikolaos Kynatidis[1], Christos Michail[1], Ioannis Seferis[2], Ioannis Valais[1], Nektarios Kalyvas[1], George Fountos[1] and Ioannis Kandarakis[1]

[1]Laboratory of Ionizing and Non Ionizing Radiation Imaging Systems, Department of Medical Instruments Technology, Technological Educational Institute of Athens 12210 Egaleo, Athens, Greece

[2]University of Patras, Department of Medical Physics, Medical School, 26504, Rio, Patras, Greece

e-mail: kandarakis@teiath.gr

Abstract. *Fundamental imaging performance in terms of Modulation Transfer Function (MTF) was investigated for a high resolution CMOS based imaging sensor and a commercial Computed Radiography (CR) unit. The CMOS device consists of a 33.91 mg/cm^2 Gd$_2$O$_2$S:Tb scintillating screen, placed in direct contact with a CMOS photodiode array. The CMOS photodiode array, featuring 1200×1600 pixels with a pixel pitch of 22.5 µm , was used as an optical photon detector. The MTF was measured using the slanted-edge method (measuring the Edge Spread Function–ESF), as well as by using pin-hole phantoms (measuring the Point Spread Function–PSF). The experimental procedure was performed under the representative radiation quality (RQA) settings, RQA 5 (70 kVp digital radiography) and RQA M2 (28 kVp digital mammography) recommended by the International Electrotechnical Commission Reports 62220-1 and 62220-1-2 respectively. It was found that the detector response function was linear for the exposure ranges under investigation. MTF for the pin-hole method was found to increase by diminishing pin-hole size up to the detector pitch (22.5 µm). Additionally, our results showed that for the same RQA quality, MTF was comparable in the whole spatial frequency range by both ESF and PSF (50 µm) methods. MTF of the CMOS imaging sensor was found better compared with the CR unit as well as compared with previously published data for other CCD and CMOS sensor.*

Keywords: CMOS, CR, Image Quality, MTF, Slanted-edge Method, Pin-hole Phantoms

1   INTRODUCTION

The majority of the medical digital X-ray detectors consist of two main components: an X-ray conversion layer, such as a scintillator/phosphor screen (indirect conversion) or a photoconductor (direct conversion), that transforms the incidents X-rays into light photons or electron-hole pairs respectively and an optical sensor that measures these secondary quanta. Having this separation of components in mind, modern digital projection systems can be divided into two groups, the Computed Radiography (CR) systems and the Digital Radiography (DR) systems [1],[2]. Cassette based CR systems have been established as the primary pathway from screen film to digital radiography. Although the intrinsic image quality of the present day CR systems is significantly inferior to DR systems, its broad acceptance has been due to the large dynamic range, easy portability, low cost and the contribution to the rapid spread of the PACS [3],[4]. On the other hand, DR systems, utilizing mainly hydrogenated amorphous silicon (a-Si:H) flat panel detectors (AMFPIs), CCDs or CMOS based sensors, have revolutionized digital imaging technologies. Until recently, referring to the optical sensors used in indirect conversion, CCD based detectors have dominated due to their remarkable linearity, low dark signal, low read noise and high sensitivity performances [5]. However, the implementation of the CMOS (complementary metal-oxide-semiconductor) technology in medical imaging has lately raised considerable attraction [6],[7], providing detectors with lower power consumption, lower production cost, higher dynamic range [5] and optimization for use in digital mammography imaging [8].

In this study, image quality, in terms of Modulation Transfer Function (MTF), was assessed for a Computed Radiography (CR) unit and an active pixel (APS) CMOS based imaging sensor [9] under RQA 5 and RQA M2 beam qualities, according to International Electrotechnical Commission protocols [10],[11],[12]. For the measurement of the MTF the established slanted-edge method [13],[14] was used,

measuring the Edge Spread Function (ESF), in comparison with a method developed using pin-hole phantoms, measuring the Point Spread Function (PSF). MTF of the CMOS based detector was compared with the CR unit results as well as with results of previously published studies for a CCD [15] and a passive pixel CMOS imaging sensor [16].

2 MATERIALS AND METHODS

2.1 Experimental setup and imaging conditions

The experimental procedure, on the CMOS based imaging sensor, was performed under both X-ray radiography (70 kVp) and mammography conditions (28 kVp). In the radiography energy range, the Del Medical Eureka [17] X-ray tube with a rotating tungsten (W) anode and inherent filtration 1.5 mm in aluminum (Al) was used. In the mammography energy range the X-ray tube was the Giotto IMS XM12 [18] with 0.5 mm Beryllium (Be) (window) and 0.03 mm Molybdenum (Mo) as inherent filter. The CMOS detector consisted of the active pixel (APS) CMOS Remote RadEye HR [19] optical readout device coupled directly to a Gd_2O_2S:Tb phosphor screen (Min-R 2190 with a mass thickness of 33.91 mg/cm^2), with a CMOS photodiode array format of 1200×1600 pixels and a pixel pitch of 22.5 μm. The experiments were conducted under the RQA 5 (digital radiography) and RQA M2 (digital mammography) representative radiation qualities recommended by the International Electrotechnical Commission reports 62220-1 and 62220-1-2 [10],[11],[12] respectively for the characterization of medical diagnostic X-ray equipment. The RQA 5 and RQA M2 beam qualities are achieved by adding filtration of 21 mm Al and 2 mm Al respectively. The source to detector distance (SDD) was set to 185 cm for the RQA 5 and 65 cm for the RQA M2 beam qualities as suggested by the IEC reports (at least 150 cm and 50-60 cm for the radiographic and mammographic ranges respectively). In the radiography range, the exposure rate at the surface of the CMOS detector was measured using the Wellhofer WD10 [20] calibrated dosimeter while, in the mammography range, the Victoreen Model 6000-529 [21] ion chamber combined with a Victoreen Model 4000M+ dosimeter was used for measuring the entrance surface air Kerma (ESAK).

On the Computed Radiography (CR) imaging system, the experiments were carried out under the RQA 5 beam quality. The BMI X-ray tube of the General Medical Merate [23] with a rotating tungsten (W) anode and inherent filtration 1.5 mm in aluminum (Al) was used. Incident X-rays were detected using a cassette containing a CsBr:Eu photostimulable phosphor (PSP) [3] (IP Cassette type CC, 35.4×35.4 cm – 14"×14" and a pixel pitch of 100 μm) combined with Fujifilm's FCR Capsula X [24] image reader.

2.2 Image Quality

2.2.1 Signal Transfer Property (STP)

First step in the image quality assessment is the determination of the detector response by measuring the signal transfer property (STP) [13],[14] as described in the IEC protocols [10]. This indicates the linear relationship between the impinging X-rays striking the detector surface and the output pixel values. According to the IEC protocols for digital radiography and computed radiography systems, the relationship must be linear or at least linearizable. On the detector under investigation, this was achieved by plotting the mean pixel value (MPV) of an image against the air Kerma at which the image was acquired. In both RQA 5 and RQA M2 beam qualities various tube current products were used for the detector's irradiation acquiring a digital image in each case. Subsequently, a region-of-interest (ROI) of 1×1 cm was defined and analyzed for each image. System's response curve was fitted using a linear equation of the form:

$$MPV = a + b \cdot K_a \tag{1}$$

where, K_a is the air Kerma at the detector surface and *a* and *b* are adjustable coefficients indicating the magnitude of the pixel offset at zero air Kerma and the value of the gain factor (G) from the slop of the curve respectively [24].

e-Περιοδικό Επιστήμης & Τεχνολογίας
e-Journal of Science & Technology (e-JST)

Workshop on Bio-Medical Instrumentation and related
Engineering And Physical Sciences
Technological Educational Institute of Athens
Athens 6 July 2012

2.2.2 Modulation Transfer Function (MTF)

Firstly, the MTF, which describes the capacity of the detector to transfer the modulation of the input signal to its output and is directly related to the resolution of the system [25], was measured using the slanted-edge method [13],[14] with the use of a PTW tungsten edge test device (L659136).The edge test device consists of a 1 mm thick edge plate (100×75 mm) fixed on a 3 mm thick lead plate. The edge was placed at the center of the detector at a slight angle (from 1° to 3°) and the images were obtained in both RQA 5 and RQA M2 beam qualities according to the IEC 62220-1 report [10]. Three exposure levels were chosen for the measurements, while the medium (E_{medium} = 63 mAs) level corresponds to the 'normal' level employed in the clinical practice. The other two levels correspond to $E_{medium}/3$ and $3×E_{medium}$ [10]. Square ROIs of 5×5 cm with the angle of the edge at the center were extracted from each image and edited with software developed in Matlab [26]. The angle of the edge was then determined using a simple linear least squares fit and the 2D image data were re-projected around the angled edge [27] to form an edge spread function (ESF) with a bin spacing of 0.1 pixels. The ESF was smoothed with a median filter of five bins to reduce high frequency noise and was differentiated to obtain the line spread function (LSF) [28]. Finally, the normalized LSF was Fourier transformed to give the pre-sampling MTF.

In the second place, the MTF was measured using pin-hole phantoms though the PSF method under the RQA 5 imaging conditions. Images were obtained with the use of four circular tungsten phantoms with a pin-hole at the center. The diameter of the pin-hole was $25\,\mu m$, $50\,\mu m$, $200\,\mu m$ and $400\,\mu m$ respectively. Firstly, the centre of the point image was determined (x_0, y_0 coordinates) and line profiles passing from this point were obtained covering various angles ranging from 0° to 180° with a 2° angle step. The PSF profile can be written as $PSF(\xi) = G(x_i, y_i)$ where $G(x_i, y_i)$ are the image pixel values [25]. x_i, y_i are the pixel coordinates in the horizontal and vertical axes respectively, fulfilling the line equation criteria for the following equation:

$$y = \frac{y_2 - y_1}{x_2 - x_1}(x - x_1) + y_1 \tag{2}$$

where, $x_1 = x_0 + r \cdot \sin\theta$, $x_2 = x_0 - r \cdot \sin\theta$, $y_1 = y_0 - r \cdot \cos\theta$, $y_2 = y_0 + r \cdot \cos\theta$, $0° \leq \theta \leq 180°$ and r is the half length of the line profile. The spatial resolution in the scan plane of the imaging system can be considered as isotropic, i.e. the system has rotational symmetry. Consequently, the PSF profiles in the radial directions were averaged to produce a one-dimensional (1D) PSF profile, which was calculated as [29]:

$$PSF(\xi) = \frac{\sum_{x_i}\sum_{y_i} G(x_i, y_i)}{\sum_{x_i}\sum_{y_i} 1} \tag{3}$$

where, ξ is the pixel position in horizontal axis. The averaged PSF profile was then fitted using four different functions: a Gaussian function, Eq. (4), a sum of two Gaussian functions, Eq. (5), a Lorentzian function, Eq. (6), and a hybrid (sum) of a Gaussian and a Lorentzian functions, Eq. (7) [30]:

$$f_G(x) = a \cdot e^{(-((x-b)/c)^2} \tag{4}$$

$$f_{2G}(x) = a_1 \cdot e^{(-((x-b_1)/c_1)^2} + a_2 \cdot e^{(-((x-b_2)/c_2)^2} \tag{5}$$

$$f_L(x) = a \cdot \frac{1}{1 + (x-b)/c)^2} \tag{6}$$

$$f_{GL}(x) = a_1 \cdot e^{(-((x-b_1)/c_1)^2)} + a_2(1/(1+((((x-b_2)/c_2)^2)))) \tag{7}$$

where, the parameters a_i, b_i, c_i are the amplitude, the position of the centre of the peak, and the spread of the curve respectively calculated by a software developed in Matlab [26]. Finally, the fitted PSF profile was Fourier transformed to compute the final MTF [31].

3   RESULTS AND DISCUSSION

Figure 1 shows the CMOS based imaging sensor response curve (STP) under the RQA 5 (70 kVp) and RQA M2 (28 kVp) imaging conditions. The detector was found to have linear response in the whole exposure range. The gain factor (G), determined with the use of flat-field images, was estimated to be 0.355 and 2.289 digital units per μGy for the RQA 5 and RQA M2 beam qualities respectively. The pixel value offset was found to be 8.58 and -0.05 and the correlation coefficient (R^2) 0.9986 and 0.9972 respectively. The tube current-time products were set at: 20, 63 and 157 mAs for the RQA 5 beam quality and 20, 60 and 120 mAs for the RQA M2 beam quality.

Figure 2 demonstrates the MTF curves for the RQA 5 and RQA M2 at 34.36 μGy and 20.29 μGy respectively. The MTF curve for the RQA M2 appears to be higher than the MTF curve for the RQA 5 beam quality. Specifically, at lower spatial frequencies the differences in the MTF values are higher. The possible explanation for this is the fact that the detector's Min-R 2190 screen is optimized for mammography applications [2], i.e., the specific screen thickness has been accepted as a compromise between resolution and light output for the RQA M2 beam quality.
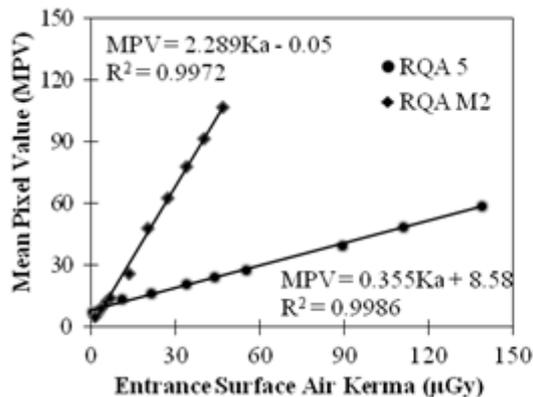
Fig. 1: STP curves for RQA 5 and RQA M2 beam qualities.
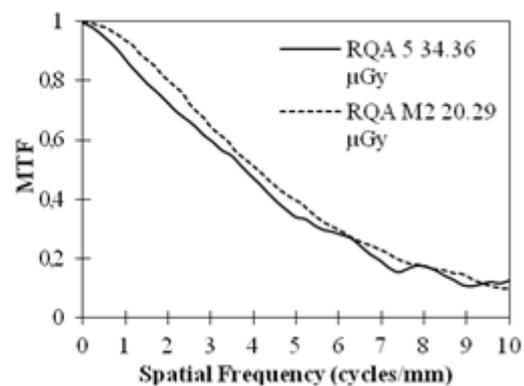
Fig. 2: MTF curves for the RQA M2 (20.29 μGy) and RQA 5 (34.36 μGy) beam qualities.

In figure 3 the MTF curve of the active CMOS sensor under investigation is being compared with the MTF curves of a passive pixel CMOS sensor and a monolithic CCD sensor, measured in previous studies [15],[16]. All measurements are obtained under the same RQA M2 beam quality for comparison purposes. MTF curve of the active CMOS sensor appears to be higher than Elbakri passive CMOS sensor [16] in the whole spatial frequency range (0-10 cycles/mm). MTF curve of the CCD sensor is lower for frequencies up to 6 cycles/mm and for higher frequencies MTF values appear to be comparable. Active CMOS sensor's supremacy is probably attributed to the smaller pixel pitch (22.5 μm compared to the 50 and 39 μm pixel pitch respectively). In addition, the detector under investigation incorporates a thinner GD_2O_2S:Tb phosphor screen, instead of the structured CsI:Tl screen with a mass thickness of 55 mg/cm^2 incorporated in the other two detectors.

e-Περιοδικό Επιστήμης & Τεχνολογίας
e-Journal of Science & Technology (e-JST)

Workshop on Bio-Medical Instrumentation and related
Engineering And Physical Sciences
Technological Educational Institute of Athens
Athens 6 July 2012
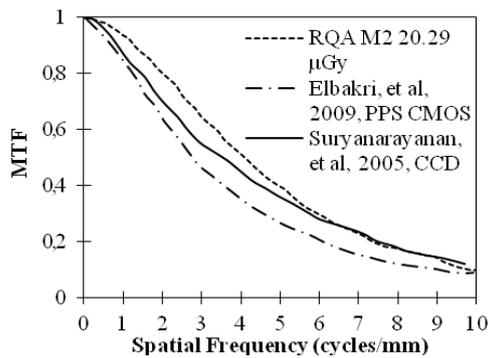
Fig. 3: Comparison between the MTF curves of the CMOS detector under investigation, a passive CMOS sensor and a CCD sensor for RQA M2 beam quality.
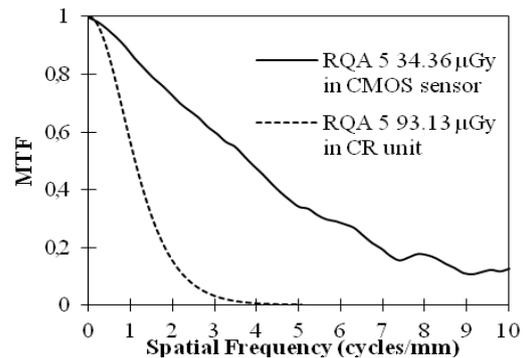
Fig. 4: MTF curves for the CMOS sensor (34.36 μGy) and the CR unit (93.13 μGy) for the RQA 5 beam quality.

Figure 4 demonstrates the MTF curves of the CMOS sensor at 34.36 μGy and the Computed Radiography (CR) unit at 93.13 μGy for the RQA 5 beam quality. Specifically, MTF curve of the CR unit appears much lower probably because of the four times larger pixel pitch of the detector (100 μm pixel pitch for the CR unit instead of the 22.5 μm pixel pitch of the CMOS sensor).

Figure 5 illustrates the MTF curves of the CMOS sensor calculated by measuring the Point Spread Function (PSF) for the RQA 5 beam quality at 63.65 μGy. PSF was measured with the use of four circular pin-hole phantoms with different pin-hole diameter. The 25 μGy diameter pin-hole phantom was not included in the results since a PSF profile was not feasible to be obtained. This was related to the extremely small pin-hole size along with the appearance of aliasing effects in the extracted image. In figure 5 the MTF curve measured by the image appearing the 50 μm pin-hole phantom appears to be higher than the other two curves. Particularly, it was found that, using the pin-hole method, MTF increases by diminishing pin-hole size up to the detector pixel pitch (22.5 μm).
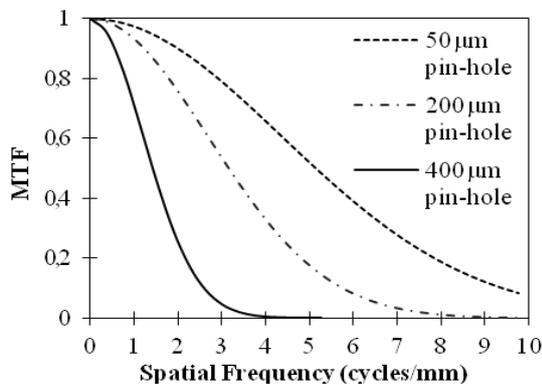
Fig. 5: MTF curves by measuring PSF using pin-hole phantoms of 50, 200 and 400 μm diameter respectively method for the RQA 5 (63.65 μGy) beam quality.
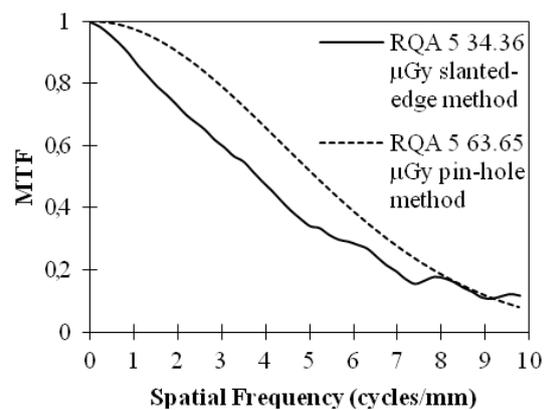
Fig. 6: Comparison of the MTF curves of the slanted-edge (34.36 μGy) and the pin-hole (63.65 μGy) for the RQA 5 beam quality.

Figure 6 shows the comparison between MTF curves using the widely established slanted-edge method and the pin-hole method for RQA 5 imaging conditions. For the pin-hole method, the MTF curve of the 50 μm pin-hole phantom was used due to the fact that it appeared the higher MTF values. The MTF curve of the pin-hole method appears to be higher up to the 9 cycles/mm while at higher frequencies the MTF values appear to decrease.

4 CONCLUSIONS

The Modulation Transfer Function (MTF) of a CMOS based imaging sensor and a Computed Radiography (CR) unit was evaluated. MTF was measured using both slanted-edge method by measuring the ESF and pin-hole phantoms by measuring the PSF. MTF of the CMOS sensor, using the slanted-edge method was higher compared to the CR unit as well as to previously published data for other CCD and PPS CMOS sensor. Additionally, MTF, using the pin-hole method, was found to increase by diminishing pin-hole size up to the detector pixel pitch (22.5 *μm*). Comparing the two methods under the same RQA beam quality, MTF of the CMOS imaging sensor was comparable in the whole spatial frequency range. These results indicate that the implementation of the pin-hole phantoms for the MTF evaluation of digital imaging systems could constitute a plausible alternative method and is worthwhile of further investigation.

ACKNOWLEDGMENTS

REFERENCES

[1] J. Yorkston, "Recent developments in digital radiography detectors", *Nuclear Instruments and Methods Research A*, 580, pp. 974-985, 2003.

[2] M. J. Yaffe, "Digital mammography, in *Handbook of Medical Imaging Physics and Psychophysics*, J. Beutel, H. L. Kundel, and R. L. Van Metter, Eds. Bellingham, WA: SPIE, vol. 1, ch. 5, pp. 329–372, 2000.

[3] J. A. Rowlands, "The physics of computed radiography", *Phys. Med. Biol.*, 47, pp. R123-R166, 2002.

[4] A. R. Cowen, A. G. Davies, S. M. Kengyelics, "Advances in computed radiography systems and their physical imaging characteristics", *Clinical Radiology,* 62, pp.1132-41, 2007.

[5] M. Nikl, "Scintillation detectors for x-rays", *Meas. Sci. Technol*., vol. 17, pp. R37–R54, 2006.

[6] M. Bigas, E. Cabruja, J. Forest, and J. Salvi, "Review of CMOS image sensors", *Microelectron. J.*, vol. 37, pp. 433–451, 2006.

[7] H. G. Chotas, J. T. Dobbins III and C. E. Ravin, "Principles of digital radiography with large-area, electronically readable detectors: A review of the basics", *Radiology*, vol. 210, pp. 595–599, 1999.

[8] C. Michail, et al., "Experimental and Theoretical Evaluation of a High Resolution CMOS Based Detector Under X-Ray Imaging Conditions", *IEEE Transactions On Nuclear Science,* 58(1), pp.314-22, 2011.

[9] C. D. Arvanitis, et al., "Empirical electro-optical and X-ray performance evaluation of CMOS active pixels sensor for low dose, high resolution X-ray medical imaging", *Med. Phys*., 34(12), pp.4612-25, 2007.

[10] IEC 62220-1-2, "Medical Electrical Equipment-Characteristics of Digital X-Ray Imaging Devices-Part 1–2: Determination of the Detective Quantum Efficiency-Mammography Detectors IEC", International Electrotechnical Commission, Geneva, Switzerland, 2005.

[11] IEC 61267, "Medical Diagnostic X-ray Equipment-Radiation Conditions for use in the Determination of Characteristics IEC", International Electrotechnical Commission, Geneva, Switzerland, 1994.

[12] sIEC 61267, "Medical Diagnostic x-Ray Equipment-Radiation Conditions for Use in the Determination of Characteristics", International Electrotechnical Commission, Geneva, Switzerland, 2003.

[13] N. W. Marshall, "A comparison between objective and subjective image quality measurements for a full field digital mammography system", *Phys. Med. Biol.,* 51, pp.2441–63, 2006a.

[14] E. Samei, , M. J. Flynn and D. A. Reimann, "A method for measuring the presampled MTF of digital radiographic systems using an edge test device", *Med. Phys.,* 25, pp.102–13, 1998.

[15] S. Suryanarayanan, A. Karellas, S. Vedantham and S. K. Onishi, "High-resolution imager for digital mammography: Physical characterization of a prototype sensor", *Phys. Med. Biol.,* 50, pp.3957–69, 2005.

[16] I. A. Elbakri, B. J. McIntosh and D. W. Rickey, "Physical characterization and performance comparison of active- and passive-pixel CMOS detectors for mammography", *Phys. Med. Biol.,* 54, pp.1743–55, 2009.

[17] Del Medical Systems Group, Roselle IL, [online] available at: http://www.delmedical.com

[18] IMS Giotto Image, Analog Mammography, Bologna, Italy, [online] available at: http://www.imsitaly.com/eng/giottoimage.htm

[19] RadEye[TM], Rad-icon Imaging Corp., USA, [online] available at: http://www.radicon.com/pdf/Remote_RadEye_Product_Family.pdf

[20] Wellhofer Dosimetrie, Wellhofer WD 10 with detector H / DN – 2 X, ISO 9001 certified, [online] available at: http://www.elimpex.com/companies/ scanditonixwellhoefer/wd10.htm

[21] Fluke Biomedical, Victoreen® X-Ray Test Device, Model 4000M+, Everett, WA, USA, [online] available at: http://www.flukebiomedical.com/Biomedical/usen/Diagnostic-Imaging-QA/X-RayQAInstruments

[22] General Medical Merate, BMI, Seriate, Italy, [online] available at: http://www.gmmspa.com

[23] Fujifilm Global, FCR Capsula X Image reader, Fuji Computed Radiography, Tokyo, Japan, [online] available at: http://www.fujifilm.com/products/medical/products/computed_radiography/capsula_x

[24] U. Neitzel, S. Gunther-Kohfahl, G. Borasi and E. Samei, "Determination of the detective quantum efficiency of a digital x-ray detector: Comparison of three evaluations using a common image data set", *Med. Phys.*, vol. 31, pp. 2205–2211, 2004.

[25] H. Fujita, et al., "A simple method for determining the modulation transfer function in digital radiography", *IEEE Trans. Med. Imaging*, 11, 34-39, 1992.

[26] MathWorks, *MATLAB*, version 7.01, computer program, The MathWorks Inc., Natick, MA, USA, 2004.

[27] N. W. Marshall, "Comparison between objective and subjective image quality measurements for a full field digital mammography system", *Phys. Med. Biol.,* vol. 51, pp. 2441–63, 2006b.

[28] N. W. Marshall, "Early experience in the use of quantitative image quality measurements for the quality assurance of full field digital mammography x-ray systems", *Phys. Med. Biol.*, vol. 52, pp. 5545–5568, 2007.

[29] Z. Chen and R. Ning, "Three-dimensional point spread function measurement of cone-beam computed tomography system by iterative edge blurring algorithm", *Phys. Med. Biol*., 49, 1865-1880, 2004.

[30] J. A. M. Santos, et al., "Single-acquisition method for simultaneous determination of extrinsic gamma-camera sensitivity and spatial resolution", *Appl. Rad. Isot*., 66(1), 44-49, 2008.

[31] M. J. Boone, "Determination of the presampled MTF in computed tomography", *Med. Phys*., 28, 356-360, 2001.